Fifth International Conference on CFD in the Process Industries
CSIRO, Melbourne, Australia
13-15 December 2006

STIRRING OF MELTS USING ROTATING AND TRAVELLING MAGNETIC FIELDS

Jörg STILLER[1], Kristina KOAL[1], Karel FRAŇA[2] and Roger GRUNDMANN[1]

[1] TU Dresden, Institute for Aerospace Engineering (ILR), 01062 Dresden, GERMANY
[2] University Liberec, Faculty of Mechanical Engineering, 46117 Liberec 1, CZECH REPUBLIC

ABSTRACT

Electromagnetic stirring provides an attractive approach to control the melt flow in metallurgy and crystal growth. Recently, the combination of rotating and travelling magnetic fields has received much interest. While the laminar flow driven by the individual fields is well investigated, the turbulent regime and the effects of superposition are largely unexplored. The paper presents numerical simulations for different combinations of rotating and travelling fields. The numerical model is based on the low-frequency / low-induction limit and employs a spectral element – Fourier method for spatial discretisation. Our results indicate that a travelling field superimposed to a rotating magnetic field leads to an intensification of swirl and secondary flow on one side, opposed by an even more significant breaking effect on the other side. A direct numerical simulation performed for stronger forcing revealed a similar scenario for the turbulent case.

NOMENCLATURE

B	magnetic induction
f	Lorentz force
j	electric current density
H	cylinder height
k	wave number
p	pressure
r	radius
R	cylinder radius
u	velocity
z	axial position originating from the center
ν	kinematic viscosity
ρ	density
σ	electric conductivity
φ	azimuth angle
ω	angular frequency

INTRODUCTION

Electromagnetic stirring is widely used to control the melt flow in metallurgy and crystal growth, although the objectives are rather different. In crystal growth processes one intends to enhance the convective transport while maintaining a stable laminar flow. In metallurgical applications the focus lies on the efficient mixing of the melt, which implies that the flow is usually turbulent.

Among the variety of oscillating magnetic fields, two are of particular interest for stirring, namely the rotating magnetic field (RMF) and the travelling magnetic field (TMF). Similar to an induction motor, an RMF generates a swirling motion in the melt. The effect of a TMF can be compared with a linear motor. The base flow driven by a TMF in a finite cylinder can be characterised by a single toroidal vortex.

Although rotating and travelling fields have been routinely used in industrial applications (Tsavaras and Brody, 1984, Davidson, 1999, Spitzer and Pesteanu, 2000), the physics of the induced flows is not yet fully understood. Various studies dealt with the properties and stability of the laminar flow driven by an RMF (Gelfgat and Priede, 1995, Davidson, 1999, Grants and Gerbeth, 2001-2003) or TMF (Ramachandran et al., 2000, Grants and Gerbeth, 2004, Yesilyurt et al., 2004), respectively. The nature of the turbulent flow regimes is largely open. So far, we are aware of only one study providing details on the transitional and weakly turbulent flow driven by an RMF (Stiller, Fraňa and Cramer, 2006).

Several authors investigated the influence of a rotating field on the solidification of metal alloys. Roplekar and Dantzing (2001) and Willers et al. (2005) demonstrated that the application of an RMF can promote the columnar-to-equiaxed transition in binary alloys. Unfortunately, the topology of the secondary flow and the occurrence of Taylor-Görtler (TG) vortices cause some unfavourable side effects such as macrosegregations as well as layered substructures in the peripheral region of the alloy (Nikrityuk et al., 2006). In order to eliminate these drawbacks, the application of travelling and superimposed fields is under consideration.

This paper presents a numerical study of the flow induced by the superposition of travelling and rotating fields for the case of a cylindric geometry. To understand the main effects, the laminar flow was investigated for combinations with differing intensities of the individual fields. For one case, the turbulent flow resulting at higher forcing was studied by means of direct numerical simulation.

MATHEMATICAL MODEL

Configuration

We consider the isothermal flow of an electrically conducting fluid in finite cylinder with diameter $D = 2R$ and height H. The flow is driven either by an RMF, a TMF or a combination of both (see Fig. 1 for a sketch). Practical applications of stirring use low-frequency fields and are characterized by relatively small fluid velocities. Therefore, it is appropriate to adopt the low-frequency / low-induction limit, in which shielding effects and flow-induced electric currents are negligible.

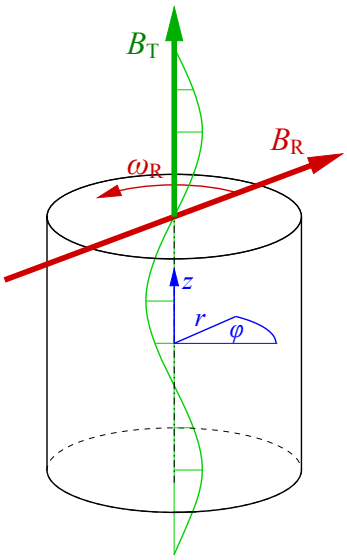

Figure 1: Geometric configuration and applied fields.

Electromagnetics

Rotating magnetic field

The RMF is characterized by the induction

$$\mathbf{B}_R = B_R[\cos(\varphi-\omega_R t)\mathbf{e}_r - \sin(\varphi-\omega_R t)\mathbf{e}_\varphi] \quad (1)$$

and the current density

$$\mathbf{j}_R = \sigma(\mathbf{E}_R - \nabla\Phi_R) \quad (2)$$

where

$$\mathbf{E}_R = \omega_R B_R r\cos(\varphi-\omega_R t)\mathbf{e}_z$$

is the induced electric field and

$$\Phi_R = \omega_R B_R \sum_{n=1}^{\infty} \frac{2J_1(\lambda_n r/R)\sinh(\lambda_n z/R)}{\lambda_n(\lambda_n^2-1)J_1(\lambda_n)\cosh(\lambda_n H/D)} r^2\cos(\varphi-\omega_R t)$$

the electric potential, J_1 is the Bessel function and the λ_n are the zeros of J_1' (Gorbachev et al., 1974).

Travelling magnetic field

We restrict ourselves to long-wave TMFs ($kH \ll 1$), for which according to Grants and Gerbeth (2004)

$$\mathbf{B}_T = B_T[\tfrac{1}{2}kr\sin(\varphi-\omega_T t)\mathbf{e}_\varphi + \cos(\varphi-\omega_T t)\mathbf{e}_z] \quad (3)$$

and

$$\mathbf{j}_T = \tfrac{1}{2}\sigma\omega_T B_T r\sin(kz-\omega_T t)\mathbf{e}_\varphi\,. \quad (4)$$

Lorentz force

The electromagnetic body force resulting from the superposition of a rotating and a travelling field is given by

$$\mathbf{f} = \mathbf{j}_R\times\mathbf{B}_R + (\mathbf{j}_R\times\mathbf{B}_T + \mathbf{j}_T\times\mathbf{B}_R) + \mathbf{j}_T\times\mathbf{B}_T = \mathbf{f}_R + \mathbf{f}_S + \mathbf{f}_T\,.$$

The contributions of the individual fields, $\mathbf{f}_R$ and $\mathbf{f}_T$, can be decomposed into a mean part and a fluctuation part with the double angular frequency, $2\omega_R$ and $2\omega_T$, respectively. Typically, these frequencies are much higher than the characteristic frequency of the flow, $\omega_F = u_{max}/R$. Hence, the corresponding forces can be approximated by the average over one period of oscillations:

$$\mathbf{f}_R = \frac{\sigma\omega_R B_R^2 r}{2}\phi(r/R, z/R, H/D)\mathbf{e}_\varphi \quad (5)$$

with the shape function

$$\phi(r,z,h) = 1 - \frac{1}{r}\sum_{n=1}^{\infty}\frac{2J_1(\lambda_n r)\cosh(\lambda_n z)}{(\lambda_n^2-1)J_1(\lambda_n)\cosh(\lambda_n h)} \quad (6)$$

and

$$\mathbf{f}_T = \frac{\sigma\omega_R B_T^2 kr}{8}\mathbf{e}_z\,. \quad (7)$$

The third contribution, $\mathbf{f}_S$, emerges from the interaction of each field with the currents induced by the other one. The resulting body force oscillates with the combination frequencies $\omega_R \pm \omega_T$. In the scope of this work we assume that the difference between ω_R and ω_T is still large in comparison with ω_F such that $\mathbf{f}_S$ can be neglected.

Flow equations

Using the scales R^2/ν, R, ν/R, and $\rho\nu^2/R^3$ for time, length, velocity, and body force, the flow equations can be written in non-dimensional form as

$$\nabla\cdot\mathbf{u} = 0 \quad (8)$$

$$\partial_t\mathbf{u} + \nabla\cdot\mathbf{uu} = -\nabla p + \nabla^2\mathbf{u} + f_R\mathbf{e}_\varphi + f_T\mathbf{e}_z \quad (9)$$

with the body forces

$$f_R = \mathrm{Ta}\, r\phi(r,z,h) \quad (10)$$

$$f_T = \tfrac{1}{2}\mathrm{F}\, r^2 \quad (11)$$

where $h = H/D$ is the aspect ratio,

$$\mathrm{Ta} = \frac{\sigma\omega_R B_R^2 R^4}{2\rho\nu^2} \quad (12)$$

the magnetic Taylor number of the RMF and

$$\mathrm{F} = \frac{\sigma\omega_T B_T^2 kR^5}{4\rho\nu^2} \quad (13)$$

the forcing parameter of the TMF.

NUMERICAL METHOD

All numerical simulations presented here are based on the spectral element – Fourier spectral code *semtex* developed at CSIRO Melbourne by H.M. Blackburn. The underlying discretisation method employs quadrilateral nodal elements in the meridional semi-plane, coupled with trigonometric expansions in the azimuth. For details of the method we refer to (Blackburn and Sherwin, 2004). The implementation of the Lorentz forces for rotating and travelling magnetic fields was verified by comparison with the linear stability analysis provided by Grants and Gerbeth (2002, 2003).

RESULTS

Laminar flow

Figure 2 shows the axisymmetric flow that is generated by an RMF (left) and by a TMF (right) in a cylinder of aspect ratio one. In both cases, the forcing parameter is chosen approximately 20% below the linear stability threshold, $\mathrm{Ta_c} = 123200$ and $\mathrm{F_c} = 120400$, respectively (Grants and Gerbeth, 2002, 2003). The interaction of the RMF-driven swirling flow with the vertical boundaries leads to the formation of Bödewadt (or Ekman) layers, which drive a meridional secondary flow consisting of two toroidal vortices. In case of the TMF, the base flow represents a single toroidal vortex moves the fluid upwards at the rim and returns it through the centre of the cylinder.

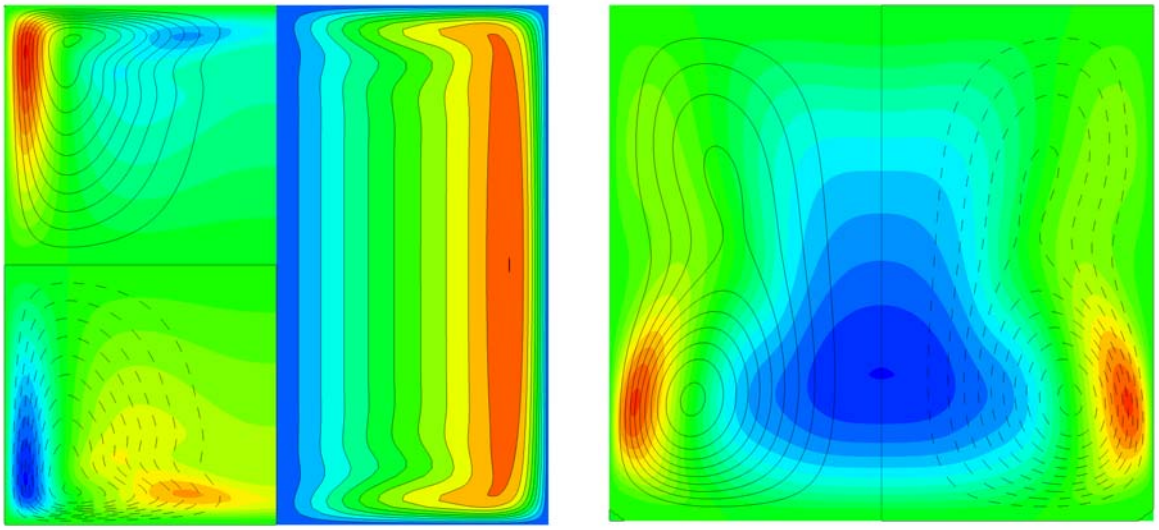

(a) Flow driven by a rotating magnetic field at $Ta = 10^5$. Left side: streamlines in the meridional semi-plane, colour indicates magnitude of vertical velocity (blue downward, red upward). Right side: Magnitude of azimuthal velocity.

(b) Flow driven by a travelling magnetic field at $F = 10^5$: streamlines and magnitude of the vertical velocity component.

Figure 2: Laminar flow driven by a rotating field (a) and by a travelling field (b).

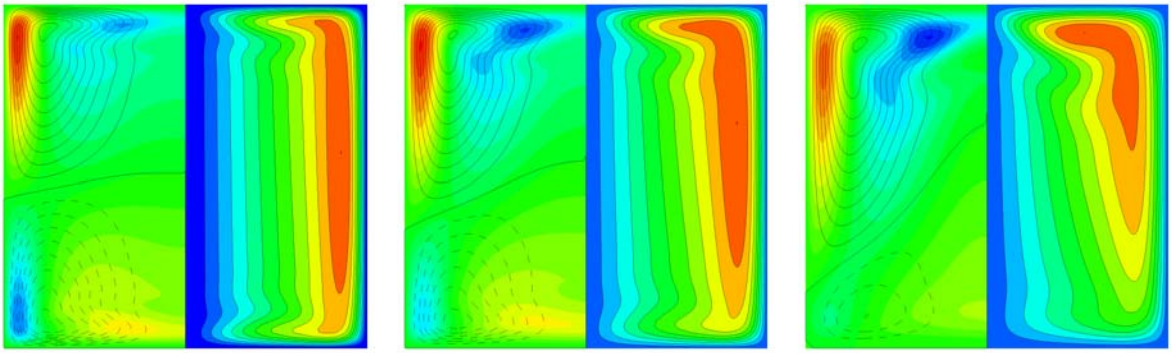

(a) Ta = 100000 (b) Ta = 50000 (c) Ta = 25000

Figure 3: Flow driven by a superposition of a travelling field with $F = 10^5$ and a rotating field with varying intensity.

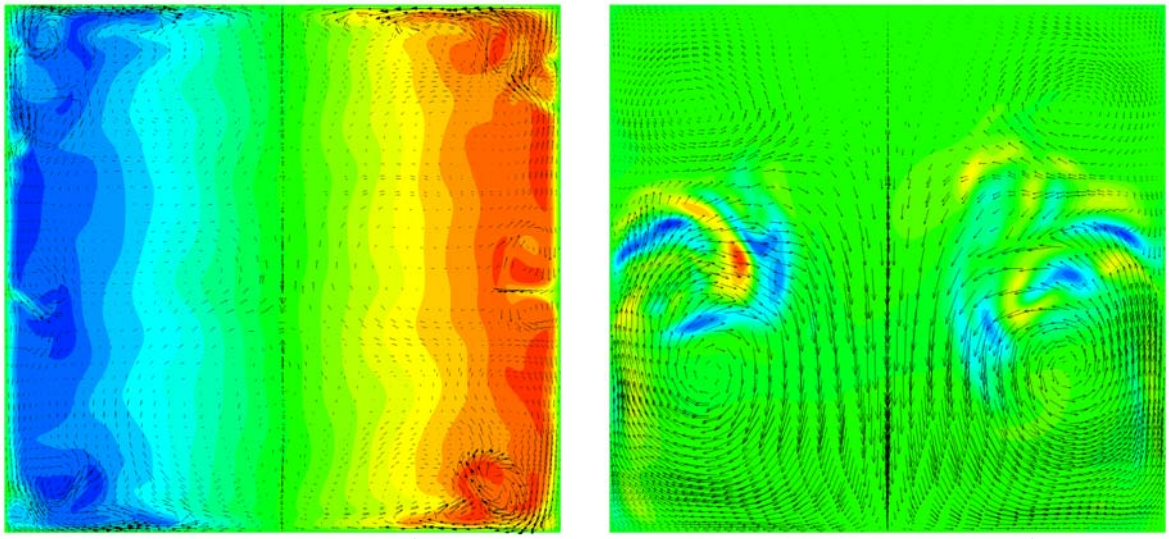

(a) Snapshot of the RMF-driven flow at $Ta = 10^6$.

(b) Snapshot of the TMF-driven flow at $F = 4\times10^6$.

Figure 4: Turbulent flow driven by a rotating field (a) and by a travelling field (b). Colour indicates the magnitude of azimuthal velocity, vectors depict the meridional velocity.

The magnitude of velocities induced at near-critical conditions by the RMF exceeds that induced by the TMF by a factor of approximately three. Therefore, it is not surprising that flow generated by the superposition of both fields is dominated by the effect of the RMF (Fig. 3(a)). In Figures 3(b-c) the intensity of the rotating field was reduced to $Ta = 5\times10^5$ and 2.5×10^5, respectively. In the latter case, the velocities induced by the individual fields are comparable. The primary effects of the superposition of the travelling with the rotating field are the following: First, the swirling motion of the fluid is intensified in the upper part of the cylinder. The upward motion forced by the TMF near the rim leads to an enhanced vertical transport of angular momentum, which is produced mainly in the middle part of the cylinder. As a consequence, the maximum of the azimuthal velocity is shifted from the middle section into the Bödewadt layer at the upper lid. This effect can be of interest for the control of solidification processes. In addition, the meridional flow intensifies locally. The peak values of the axial and radial velocity components increase from 14 to 34 and 30 to 50 percent of the azimuthal velocity. At the same time the flow is significantly decelerated in the lower part of the cylinder.

Turbulent flow

In metallurgic applications of electromagnetic stirring, the turbulent regime is usually preferred, because it provides a better mixing of the melt. However, except for the case of an RMF (Stiller, Fraňa and Cramer, 2006), the turbulent flow induced by alternating magnetic fields is scarcely investigated. In this study, direct numerical simulations (DNS) were carried out for an RMF with $Ta = 10^6$, a TMF with $F = 4\times10^6$, and the superposition of these fields. The computations employed a non-equidistant grid of 25×50 elements with a polynomial degree of 11, and 128 planes in the azimuthal direction (approx. 20 million DOF per variable). The corresponding grid resolution varied from $\Delta^+ \le 0.21$ at the walls to $\Delta^+ \le 3.5$ in the core region (in viscous units).

Figure 4(a) depicts a snapshot of the flow driven by the rotating field. Except for the Bödewadt layers and the effect of large-scale fluctuations, the swirl distribution is almost homogeneous in the axial direction. In previous studies (Fraňa, Stiller and Grundmann, 2005, Stiller, Fraňa and Cramer, 2006) it was shown that, apart from oscillations of the rotation axis, Taylor-Görtler (TG) vortices represent the major turbulence mechanism in the RMF-driven flow. Both mechanisms are present also in the snapshot shown in Fig. 4(a). In a recent work Nikrityuk, Eckert and Grundmann (2006) demonstrated that the presence of TG vortices leads to a dramatic improvement of the mixing efficiency.

Figure 4(b) shows a snapshot of the velocity field for the travelling field. Here, the main flow consists of two toroidal vortices, as opposed to only one in the laminar case (compare Fig. 2(a)). The inspection of further snapshots revealed that this configuration is only one in a sequence of flow patterns with different topologies. While the detailed investigation of this process is still in progress, it can be stated that the turbulent flow driven by the TMF is far less regular than in case of the RMF. The peak velocities in the TMF reach about one half of those in the RMF, whereas the turbulent kinetic energy is of the same order.

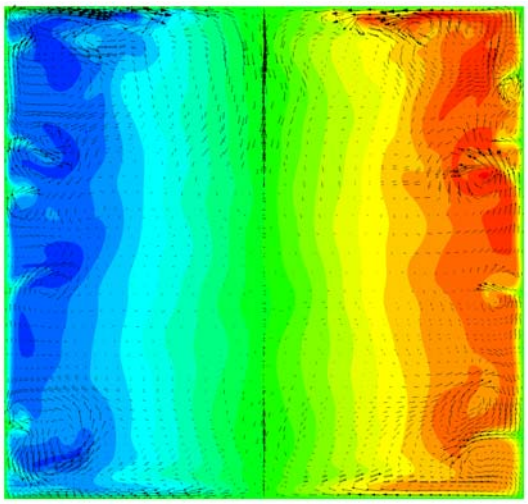

Figure 5: Snapshot of the turbulent flow for $Ta = 10^6$ and $F = 4\times10^6$. Colour indicates the intensity and direction of azimuthal flow, vectors the meridional flow.

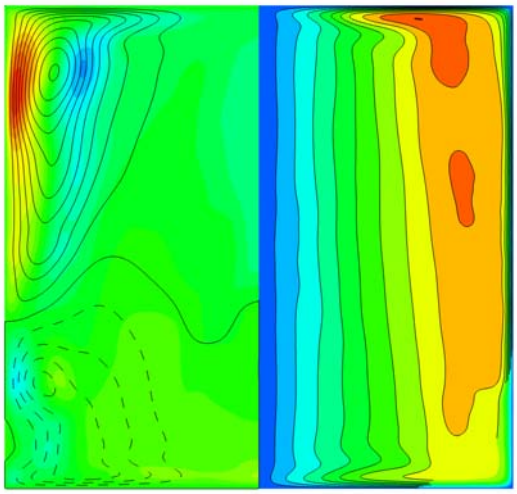

Figure 6: Average velocity at $Ta = 10^6$ and $F = 4\times10^6$. For caption see Fig. 2(a).

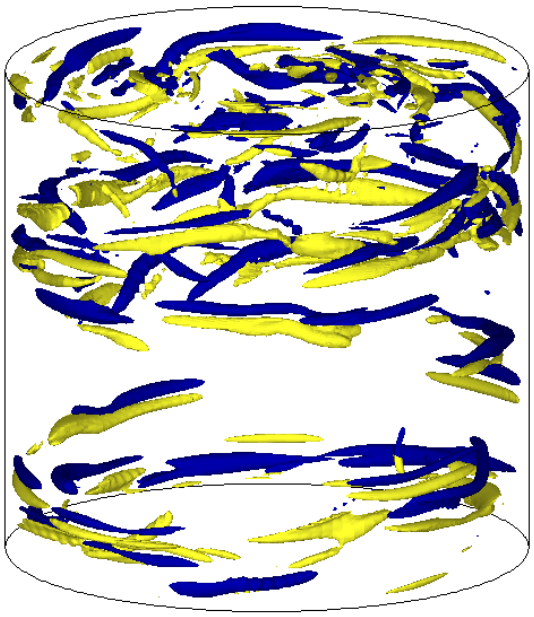

Figure 7: Vortices visualised with the λ_2 criterion (Jeong and Hussain, 1998).

Finally we consider the superposition of the fields. The snapshot shown in Figure 5 resembles the RMF-driven flow, but reveals similar superposition effects as in the laminar case (Fig. 3(c)). The mean flow distribution depicted in Fig. 6 confirms the expected redistribution of angular momentum towards the top of the cylinder. The maximum of the azimuthal velocity is again located in the Bödewadt layer, which is considerably thinner than in the laminar case. Figure 7 illuminates the vortex structures associated with the turbulent velocity fluctuations. In comparison with the pure RMF-case (Stiller, Fraňa and Cramer, 2006), the superposition of the TMF does not introduce any new structures. Instead, the number of Taylor-Görtler vortices – and thus the turbulence intensity – is increased in the upper part of the cylinder, whereas it is significantly reduced in the lower part.

CONCLUSION

The flow driven by rotating and travelling magnetic fields was studied under the assumption that the influence of the temporally varying part of the Lorentz force is negligible. The imposition of a pure RMF always generates a homogeneously rotating main flow. In contrast, the TMF-driven flow exhibits a regular structure only in the laminar case. When superimposed on the rotating field, the TMF causes an intensification of swirl, secondary flow and turbulence in one half of the cylinder and damps the flow in the other half. The reason for these effects is seen in the enhanced transport of angular momentum that is produced in the middle region towards one of the lids. The results suggest that a better control of unidirectional solidification processes can be achieved by a tailored combination of rotating and travelling fields. Of course, this question can be finally resolved only by means of experimental investigations. Future work should also address the effects of non-stationary forcing that can be expected when the frequencies of the superimposed fields are close to each other.

ACKNOWLEDGEMENTS

The authors are grateful to Dr. H.M. Blackburn for providing the flow solver *semtex*. We thank Dr. P. Nikrityuk and Dr. A. Cramer for fruitful discussions. Financial support from Deutsche Forschungsgemeinschaft in frame of the Collaborative Research Center SFB 609 is gratefully acknowledged. The direct numerical simulation was done on an SGI Altix system based on a grant from ZIH at TU Dresden.

REFERENCES

BLACKBURN H.M. and SHERWIN, S.J., (2004), "Formulation of a Galerkin spectral element – Fourier method for three-dimensional incompressible flows in cylindrical geometries", *J. Comp. Phys.*, **197**, 759-778.

DAVIDSON, P.A., (1999), "Magnetohydrodynamics in materials processing", *Ann. Rev. Fluid Mech.*, **31**, 273-300.

GELFGAT, Y.M. and PRIEDE, J., (1995), "MHD flows in a rotating magnetic field (a review)", *Magneto-hydrodynamics*, **31**, 188-200.

GORBACHEV, L.P., NIKITIN, N.V and USTINOV, A.L., (1974), "Magnetohydrodynamic rotation of an electrically conducting liquid in a cylindricalvessel of finite dimensions", *Magnetohydrodynamics*, **10**, 406-414.

GRANTS, I. and Gerbeth, G., (2001), "Stability of axially symmetric flow driven by a rotating magnetic field in a cylindrical cavity", *J. Fluid Mech.*, **431**, 407-426.

GRANTS, I. and Gerbeth, G., (2002), "Linear three-dimensional instability of a magnetically driven rotating flow", *J. Fluid Mech.*, **463**, 229-239.

GRANTS, I. and Gerbeth, G., (2003), "Experimental study of non-normal nonlinear transition in a rotating magnetic field driven flow", *Phys. Fluids*, **15**(10), 2803-2809.

GRANTS, I. and Gerbeth, G., (2004), "Stability of melt flow due to a travelling magnetic field in a closed ampoule", *J. Cryst. Growth*, **269**, 630-638.

JEONG, J. and HUSSAIN, F., (1998), "On the identification of a vortex", *J. Fluid Mech.*, **285**, 69-94.

NIKRITYUK, P.A., ECKERT, K. and GRUNDMANN, R., (2006a), "A numerical study of unidirectional solidification of a binary metal alloy under influence of a rotating magnetic field", *Int. J. Heat Mass Transfer*, **49**, 1501-1515.

NIKRITYUK, P.A., ECKERT, K. and GRUNDMANN, R., (2006b), "Axisymmetric modelling of the mixing of two miscible liquid metals driven by a rotating magnetic field", *Conference on Turbulence and Interactions TI2006*, Porquerolles, France, May 28 – June 2, 2006.

RAMACHANDRAN, N., MAZURUK, K. and VOLZ, M.P., (2000), "Use of traveling magnetic fields to control melt flow convection", *J. Jpn. Soc. Microgravity Appl.*, **17**(2), 98-103.

ROPLEKAR, J.K. and DANTZING, J.A., (2001), "A study of solidification with a rotating magnetic field", *Int. J. Cast Met. Res.*, **14**, 79-98.

SPITZER, K.-H. and PESTEANU, O., (2000), "Application of travelling magnetic fields in metallurgy", *Proc. Int. Symp. on Electromagnetic Processing of Materials*, Nagoya, Japan, 409-414.

FRAŇA, K., STILLER, J. and GRUNDMANN, R., (2005), "Taylor-Görtler vortices in the flow driven by a rotating magnetic field in a cylindrical container", *J. Visualization*, **8**(4), 323-330.

STILLER, J., FRAŇA, K. and CRAMER, A., (2006), "Transitional and weakly turbulent flow in a rotating magnetic field", *Physics of Fluids*, **18**, 074105.

TSAVARAS, A.A. and BRODY, H.D., (1984), "Electromagnetic stirring and continuous casting – achievements, problems and goals", *J. Met.*, **167**, 31-37.

WILLERS, B., ECKERT, S., MICHEL, U. and ZOUHAR, G., (2005), „The columnar-to-equiaxed transition in Pb-Sn alloys affected by electromagnetically driven convection", *Mater. Sci. Eng. A*, **402**, 55-65.

YESILYURT, S., MOTAKEL, S., GRUGEL, R. and MAZURUK, K., (2004), "The effect of the traveling magnetic field (TMF) on the buoyancy-induced convection in the vertical Bridgman growth of semiconductors", *J. Cryst. Growth*, **263**, 80-89.